HOKKAIDO UNIVERSITY

Title	Effect of Temperature and Confining Pressure on Permeability during Deformation and Failure of Shikotsu Welded Tuff
Author(s)	Alam A.K.M., Badrula; Niioka, Masaki; Fujii, Yoshiaki et al.
Description	ARMS7: 7th Asian Rock Mechanics Symposium. The theme of the Symposium is The Present and Future of Rock Engineering. 15-19 October 2012. COEX, Seoul, Korea.
Citation	Proceedings of the 7th Asian Rock Mechanics Symposium, 7, 563-572
Issue Date	2012-10-15
Doc URL	https://hdl.handle.net/2115/56180
Type	conference paper
File Information	ARMS7,563-572.pdf

Hokkaido University Collection of Scholarly and Academic Papers : HUSCAP

Effect of Temperature and Confining Pressure on Permeability during Deformation and Failure of Shikotsu Welded Tuff

Alam A.K.M. Badrul[a*], Masaki Niioka[a], Yoshiaki Fujii[a], Jun-ichi Kodama[a] and Takayuki Sugawara[a]

[a] Rock Mechanics Laboratory, Faculty of Engineering, Hokkaido University, Japan

Keywords: THM, Permeability, Consolidation, Compression, Welded tuff

Abstract

Permeability variation during deformation and failure in triaxial test was considered for Shikotsu welded tuff. Pure water saturated cylindrical test specimens of 30 mm in diameter and length of 60 mm with constant flow rate method at 0.3 ml/min was introduced for compression, with strain rate of 10^{-5} s^{-1} on the consolidated samples under 1 MPa, 5 MPa, 10 MPa and 15 MPa for 24 hours until the axial strain reached at 10% in 22ºC and 80ºC. Permeability at the end of 15 MPa consolidation was lower than those of under 1-10 MPa. In compression (i) permeability basically decreased with slight disturbances around peak load points due to rapid volumetric change (ii) under 1 MPa the permeability was larger, compare to 5-15 MPa confining pressure at 22ºC (iii) no apparent confining pressure dependency was observed at 80ºC. The permeability was lower at 80ºC than 22ºC. However, more water flow is expected for the same pore pressure gradient at 80ºC due to lower viscosity of water.

1. Introduction

All kinds of man-made excavations are experienced of Excavation disturbed Zone (EdZ) and Excavation Damazed Zone (EDZ). These zones are important for short and long term stability of the excavations. In situ tests have been done of these zones in field scale (Emsley et al., 1997; Sugihara et al, 1999; Backblom et al., 1999; Sato T. et al., 2000; Kwon S., et al. 2008, Fujii Y. et al., 2011). Stress redistribution as well as permeability change due to excavations within the rocks is anisotropic (Backbloom et al., 1999; Wang et al., 2001; Tsang C.-F. et al., 2004). The interplay of these anisotropic processes and behavior can be addressed as Hydromechanical (HM) coupling (Rutqvist J. et al., 2003; Neuzil C.E., 2003). Thermal effect on HM property is known as Thermo Hydro Mechanical (THM) coupling. It is important for performance assessment of radioactive waste repositories which requires long term monitoring even after closure (Hudson J.A. et al., 2005; Rutqvit et al., 2005; Kwon S. et al., 2008). THM Processes of tuff, considering air permeability have been carried out in field scale (Rutqvist et al., 2005). THM coupling within rock is very important considering human activities in wide range of applications such as, coal mining and coal methane extraction, oil and gas extraction, hydrogeology and well test analysis, geothermal energy, deep well injection of liquid and solid waste, geologic storage of natural gas, geologic sequestration of CO_2 as well as in geologic processes.

The objective of this study is to clarify permeability behavior, deformation and failure of Shikotsu welded tuff as a THM process. Triaxial tests were carried out under 1-15 MPa confining pressure at 22 and 80°C measuring permeability by the constant flow method at 0.3 ml/min to accomplish the objective. Permeability behavior during deformation and failure process and influences of temperature and confining pressure on permeability are shown. Mechanisms of the permeability change is discussed based on the test results as well as microstructure of rock specimens.

2. Experiment and Theories

2.1 Specimen

For the experiments firstly we took a block of Shikutsu welded tuff, having 199.20 mm in length (side-2), 150.25 mm in width (side-1) and 395.00 mm in height (side-3) (Figure 1). The seismic velocity (P-wave) was measured with 140 kHz sensors for each side in several positions (Table 1). The velocity in side-3 was lower compared to other two sides and was marked to maintain unifomity for coring of 30 mm in diameter and 14 cm in length. The cores were then cut and polished to the parallelism of 2/100, by making the length of 60 mm and kept into an oven at 80ºC for 24 hours. Afterward a vacuum jar was used, in order to make it 100% water-saturation by submerging for 24 hours. Two-third portion of the jar was filled with pure water and made vacuum by using a vacuum-pump.

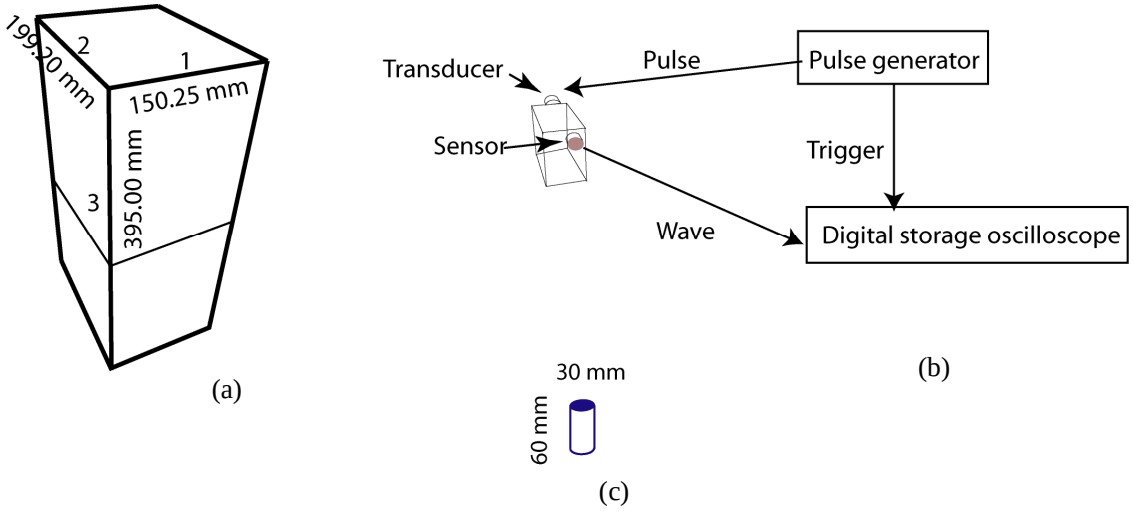


Figure 1. Specimen from block of Shikotsu welded tuff. (a) Block (b) Measuring P-wave velocity of the block (c) Specimen after coring, cutting and polishing

Table 1. P-wave velocity of the block

Block side	Length (mm)	Time (μs)	Velocity (km/s)	Average (km/s)
1	150.25	61.60	2.44	2.39
		61.60	2.44	
		65.20	2.30	
2	199.20	85.00	2.34	2.34
		86.00	2.31	
		84.60	2.35	
3	395.00	207.00	1.91	1.90
		208.00	1.90	
		208.00	1.90	
		208.00	1.90	
		207.00	1.91	

2.2 Sample preparation

Two stainless steel end-pieces having a central hole to allow the flow of water through the specimen were attached with each saturated specimen by vinyl tape. Then two cross type strain gauges were glued to the opposite sides and center of the specimen to have strain measurement. Silicone sealant was coated on the specimen upto the curvature of the end-pieces to maintain the water flow within the specimen. The heat shrinkable tube was then put into the end-piece attached specimen

(Figure 2) to prevent the specimen from direct contact of the confining fluid (water). Then the sample was kept into water of the same vacuum jar that was used to make specimen 100% water-saturation, for 24 hours.

2.3 Experiment

In the triaxial test, confining pressure (P_c) was used to make $\sigma_2 = \sigma_3$ and the axial stress (σ_A) acted as σ_1 (Figure 3(a)). In consolidation state the axial stress was made equal to the confining pressure making the stress situation as $\sigma_1 = \sigma_2 = \sigma_3$. To reach the desired consolidation pressure the axial stress was increased first, then the confining pressure was increased, up to the target consolidation pressure (Figure 3(b)).

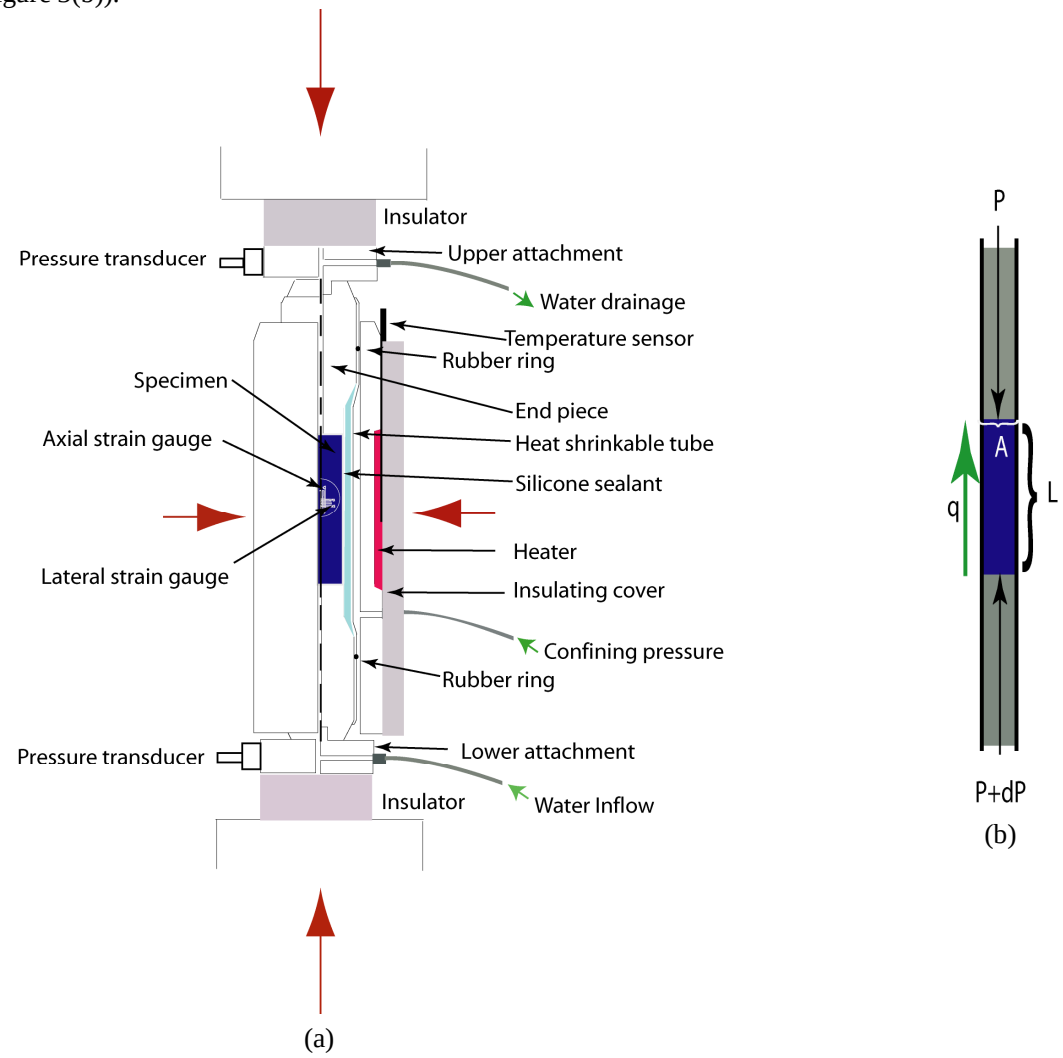


Figure 2. Experimental setup. (a) Pressure vessel with sample and accessories (b) Sketch of permeability measurement basis

In this experiment permeability measurement was carried out during triaxial test within desired consolidation pressure of 1, 5, 10, 15 MPa at 22ºC and 80ºC temperature. At the very first beginning the sample was inserted into the pressure vessel (Figure 2(a)). Then the upper and lower stainless steel attachments having the facility of water flow and measurement of pore pressure by transducer were inserted (Figure 2(a)). The lower attachment was connected to a syringe pump. The upper attachment was open to the atmosphere and used for drainage. The axial stress was introduced by using a loading frame and the confining pressure with the help of a double ball plunger pump. After reaching the target consolidation pressure, (Figure 3(b)) it kept for 24 hours in the desired temperature by using a heater, insulators and insulating cover, around the pressure vessel (Fiure 2(a)). On the consolidated

samples, constant strain rate compression was introduced at 10^{-5} s^{-1} (0.036mm/min) until the axial strain reached to 10%. During the period of the consolidation and compression, constant flow of pure water at a rate of 0.3 ml/min was maintained in the axial direction by using the syringe pump that was connected to the lower attachment (Figure 2(a)). During the experiment load, stroke, pore pessure, axial strain, lateral strain, confining pressure and the flow rate were continuously measured at a sampling interval of 10 s. After the experiments the porosity analysis was done by using the thin sectional images in software "Scion Image" of the blue resin impregnated specimens.

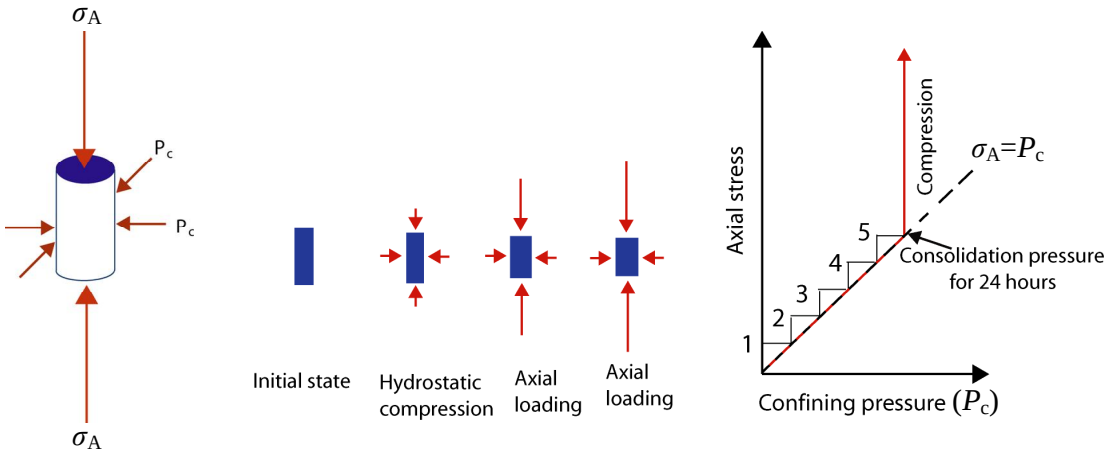


Figure 3. Triaxial test under certain consolidation pressure. (a) Triaxail test conceprt (b) Reaching the desire consolidation pressure and the compression

2.4 Calculation of Permeability

Permeability K was calculated, using the following equation having the effective porosity of the specimens at around 37% by introducing constant flow method.

$$K = \frac{q \cdot \mu}{A} \cdot \frac{\mathrm{d}L}{\mathrm{d}P} \tag{1}$$

where q is flow rate (m^3/s); μ is the fluid viscosity and it is 0.96×10^{-3} Pa·s for 22ºC, 0.35×10^{-3} Pa·s for 80ºC; A is the cross sectional area (m^2) and $\mathrm{d}P/\mathrm{d}L$ is pressure gradient (Pa/m).

3. Results and Discussion

3.1 Deformation and failure behaviour

The pore pressure, confining pressure and mode of rupture plane of the experiments are shown in Table 2 . The differntial stress-stroke based strain curves of the experiments are shown in Figure 4. The strain data from strain gauges were not able to collect for all the experiments specially not a single data for 80ºC experiments. In case of 22ºC examples of the strain gauge based strain data are plotted in Figure 5.

All specimen showed strain softening under confining pressure of 1 MPa (Figure 4(a)). Half of the specimens at 22 ºC and 80ºC belonged to strain hardening under confining pressure of 5 MPa (Figure 4(b)). Clear strain hardening was observed for all specimens under 10 and 15 MPa at 22ºC and 80ºC (Figures 4 (c) and (d)).

Increasing confining pressure, effective peak strength and tangent modulus increased (Figures 6(a) and (b)). These properties were low in high temperature. Increasing confining pressure residual strength increased nonlinearly and slightly lower at 80ºC (Figure 6(c)).

3.2 Permeability before and after compression

Increasing consolidation pressure the brittle rock became ductile in high confining pressure (Figure 4). In this figure the stress and the corresponding permeability response in the respective consolidation and deviatoric stress are shown. In all the cases in compression, permeability decreased and the decreasing magnitude was getting higher in case of higher confining pressure with slight disturbance around the peak load points because of rapid volumetric change. In most cases the permeability in 80ºC was lower than 22ºC.

Before compression (at the end of 24 hours consolidation) permeability in 15 MPa confining pressure was smaller than those of other confining pressure (Figure 7(a)). Permeability at 80ºC was slightly lower than 22ºC. After compression the permeability under 1 MPa was larger. No apparent confining pressure dependancy was observed for other conditions and permeability at 80ºC was slightly smaller than 22ºC (Figure 7(b)). From consolidation state to the end of compression in 1 MPa confining pressure small decrease of permeability was observed at 22ºC but for 80ºC the decrease was large (Figure 7(c)).

Table 2. Pore and confining pressure

Sample	Before compression		After compression		Rupture plane
	P_p (MPa)	Effective P_c $\{P_c$-$P_p/2\}$ (MPa)	P_p (MPa)	Effective P_c $\{P_c$-$P_p/2\}$ (MPa)	
T1-22A	0.17	1.07	0.10	1.05	Single
T1-22C	0.04	1.16	0.05	1.09	Single
T5-22A	0.18	5.22	0.21	5.15	None
T5-22C	0.18	5.28	0.70	5.04	None
T5-22D	0.09	5.56	0.29	5.39	None
T5-22E	0.08	5.21	0.11	5.13	None
T10-22A	0.09	10.34	0.62	9.98	None
T10-22B	0.09	10.21	0.95	9.91	None
T10-22C	0.11	10.42	0.70	10.05	None
T10-22D	0.06	10.27	0.18	10.35	None
T15-22C	0.03	15.37	0.38	15.30	None
T1-80C	0.02	1.08	0.11	1.06	Single
T5-80A	0.05	5.40	0.77	4.84	None
T5-80D	0.04	5.27	0.30	5.19	None
T10-80B	0.04	10.20	0.30	9.99	None
T10-80C	0.03	10.43	0.27	10.35	None
T10-80D	0.06	10.27	0.15	10.12	None
T15-80B	0.06	15.19	0.42	14.96	None
T15-80C	0.31	14.73	0.68	14.61	None
T15-80D	0.07	15.31	0.73	15.04	None
T1-80X	0.06	1.15			
T5-80X	0.03	5.11			
T10-80X	0.05	10.10			
T10-80Y	0.06	10.10			
T10-80Z	0.02	10.20			
T15-80X	0.09	15.10			

P_p: Pore pressure, P_c: Confining pressure, T1-22: 1 MPa 22ºC, T1-80: 1 MPa 80ºC, T5-22: 5 MPa 22ºC, T5-80: 5 MPa 80ºC, T10-22: 10 MPa 22ºC, T10-80: 10 MPa 80ºC, T15-22: 15 MPa 22ºC, T15-80: 15 MPa 80ºC, T1-80X: 1 MPa 80ºC consolidation, T5-80X: 5 MPa 80ºC consolidation, T10-80X, T10-80Y, T10-80Z: 10 MPa 80ºC consolidation, T15-80X: 15 MPa 80ºC consolidation

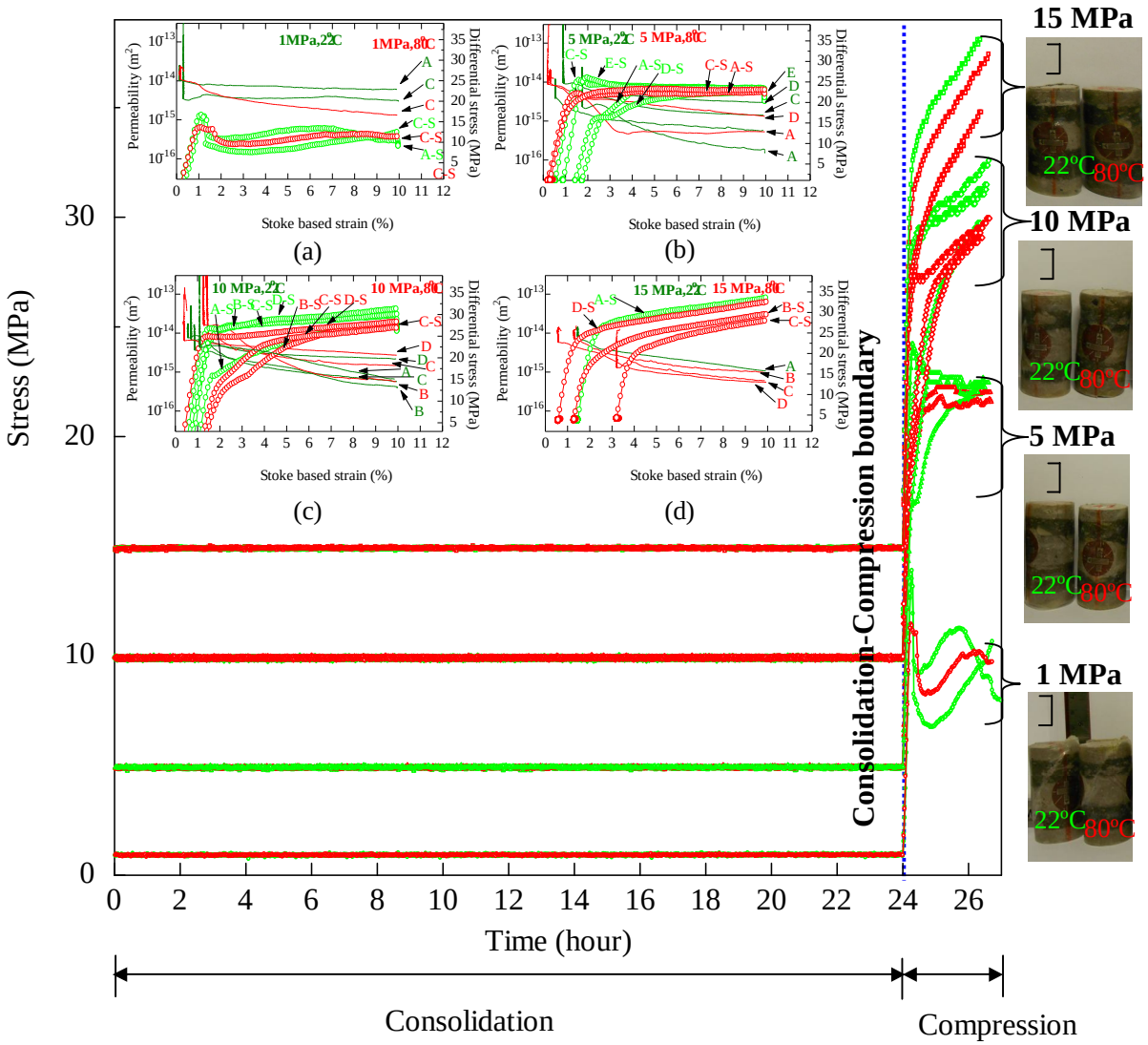


Figure 4. Permeability during consolidation and compression under different consolidation pressure. (a), (b), (c) and (d) are the permeability response under stress of 1 MPa, 5 MPa, 10 MPa and 15 MPa respectively. A-S, B-S, C-S, D-S, E-S are the stress and A, B, C, D, E are the permeability in respective cnsolidation pressure. Green lines are for 22ºC and the red lines are for 80ºC

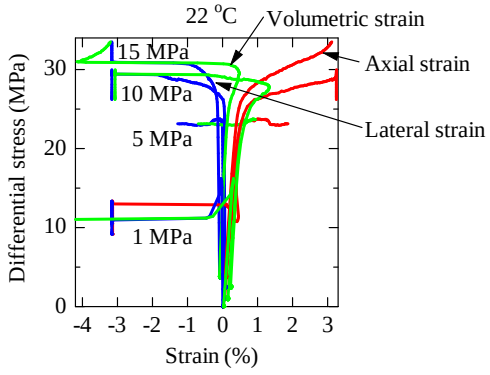


Figure 5. Example of stress-strain curves under differernt confining pressure from strain gauges.

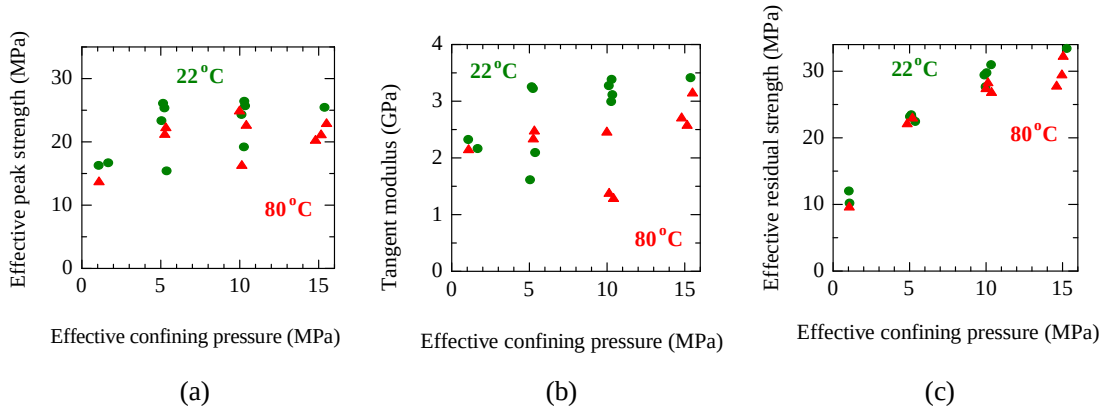


Figure 6. Mechanical properties in different confining pressure. (a) Effective strength (b) Tangent modulus (c) Effective residual strength

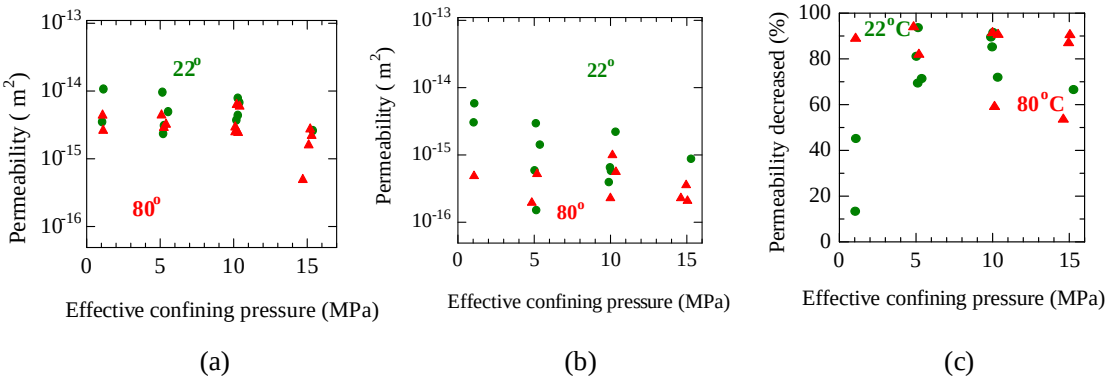


Figure 7. Consolidation and compressional effect on permeability. (a) After consolidation or deformational effect (b) After compression (c) Decreased permeability from consolidation to compression

3.3 Pore analysis

After the experiment the image analysis of the thin sections of blue resin impregnated specimens (Fiugre 8) was performed on consolidated specimens by using the software "Scion Image". The total porosity was calculated as Figure 9(a).

The porosity of 15 MPa, at 22ºC was 16.10% and for 15 MPa, at 80ºC it was 9.61%. Due to temperature effect, the porosity decreased by 40.31% (Figure 9(b)). This was because, by increasing the temperature low aspect ratio of 0.3-0.4 became dominated which was 0.5-0.6 on 22ºC (Figure 8(f)). That means in increased temperature pore became narrower.

The porosity in 1 MPa, at 80ºC was 12.00% and 9.61% in 15MPa, at 80ºC. Increasing the confining pressure in same temperature porosity decreased by 19.92% (Figure 9(b)). Increasing confining pressure pore became smaller, as in low confining pressure (1 MPa) frequency of higher equivalent diameter (0.05-0.1 mm) became smaller in number for high confining pressure of 15 MPa (Figure 8(e)). Increasing confining pressure from 1 MPa to 15 MPa and temperature from 22ºC to 80ºC in consolidation porosity decreased as the frequency of pores in all directions decreased (Figure 8(g)).

3.4 Permeability decrease as THM processes

In consolidation, increasing confining pressure from 1 to 15 MPa, at 80ºC in same temperature porosity decreased by 19.92% (Figure 9(b)). The mechanism of the permeability decrease might be

due to pore collapse because of the high confining pressure (100% UCS). By increasing temperature from 22ºC to 80ºC in same confining pressure of 15 MPa porosity decreased by 40.31% (Figure 9(b)). The pore collapse might have been accelerated by increasing in creep rate, stress corrosion, pressure solution and decrease in water viscosity etc. due to high temperature.

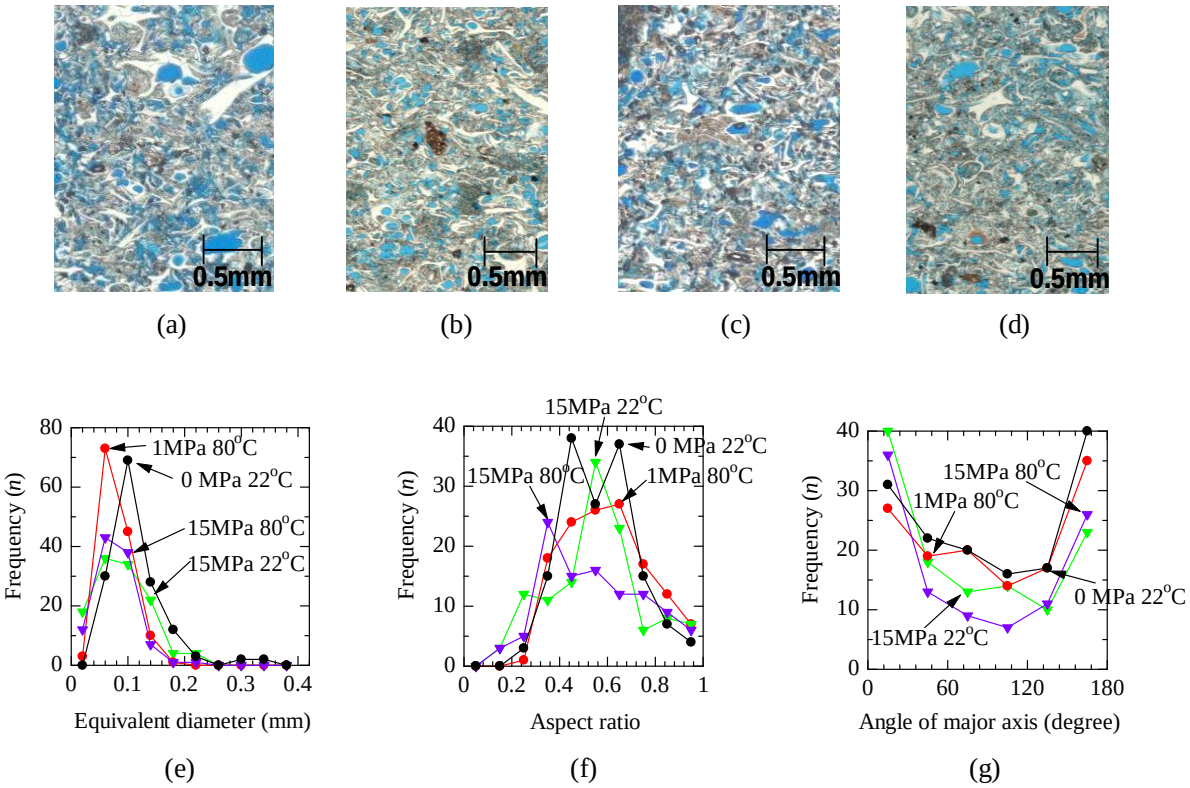


Figure 8. Pore analysis. (a), (b), (c) and (d) are thin sectional images: blue spots are the pores (e) Equivalentent diameter (f) Aspect ratio (g) Angle of major axis

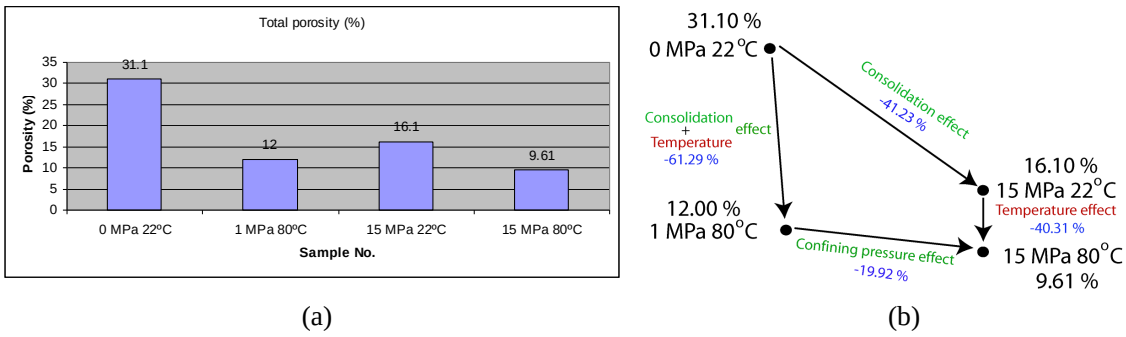


Figure 9. Toal porosity and the effect of consolidation, confining pressure and temperature. (a) Total porosity (b) Effect of consolidation, consolidation+temperature, confining pressure and temperature on total porosity

In compression permeability decreased. Whole specimens were crused except for 1 MPa cases. Smaller permeability decrease was observed in case of 1 MPa compared to other confining pressure at 22ºC. A distinct rupture plane formed under 1 MPa (Figure 4), might be the reason for the small decrease in permeability after compression at 22ºC. Permeability at 80ºC was smaller than those of 22ºC. In 80ºC temperature mineral particles around the rupture plane crushed and this might be the cause of higher magnitude of decrement in permeability at 80ºC.

4. Conclusions

In this research, laboratory experiment of permeability during deformation and failure of Shikotsu welded tuff in triaxial test was investigated. Pure water saturated 30 mm in diameter and length of 60 mm cylindrical test specimens were introduced for compression, with strain rate at 10^{-5} s^{-1} on the consolidated samples under 1 MPa, 5 MPa, 10 MPa and 15 MPa for 24 hours until the axial strain reached at 10% in 22ºC and 80ºC with constant flow rate method at 0.3 ml/min to measure the permeability. After the experiments the porosity analysis was done by using the thin sectional images in software "Scion Image" of the blue resin impregnated specimens.

Permeability at the end of 15 MPa consolidation was lower than those of under 1-10 MPa. In compression (i) permeability basically decreased with slight disturbances around peak load points due to rapid volumetric change (ii) under 1 MPa the permeability was larger, compare to 5-15 MPa confining pressure at 22ºC (iii) no apparent confining pressure dependancy was observed at 80ºC. The permeability was lower at 80ºC than 22ºC. However, more water flow is expected for the same pore pressure gradient at 80ºC due to lower viscosity of water.

The mechanism of the behaviours should be further clarified in future. The permeability response of Kimachi sandstone and Inada granite will be investigated in similar conditions.

Acknowledgement

A part of this work was supported by KAKENHI (22560804).

References

1. Backblom, G., Martin, C.D., 1999, Recent experiments in hard rock to study the excavation response: Implication of the performance of a nuclear waste geological repository, *Tunnel Underground Space Technology*, 14, 377-394.
2. Emsley, S., Olsson, O., Stenberg, L., Alheid, H.-J., Fall, S., 1997, ZEDEX- a study of damage and disturbance from tunnel excavation by blasting and tunnel boring, *Swedish Nuclear Fuel Waste Management Co (SKB), Stockholm, Tech Rep*, 30-97.
3. Fujii, Y., Sagawara, T., Kodama, J., ishijima, Y., Kiyama, T., Takada, M., Ishihara, Y., kumakura, S., narita, T., Sawada, M., Nakata, E., 2011, Abandond roadways aged up to 50 years observed in kushiro Coal Mine, Japan, *Proceedings of 12th International Congress of Rock Mechanics*, 975-978.
4. Hudson, J.A., Stephansson, O., Anderson, J., 2005, Guidance on numerical modelling of thermo-hydro-mechanical coupled processes for performance assessment of radio active waste repositories, *International Journal of Rock Mechcnics & Mining Sciences*, 42, 850-870.
5. Kwon, S., Cho, W.J., 2008, The influence of an excavation damazed zone on the thermal-mechanical and hydro-mechanical behaviours of an underground excavation, *Engineering Geology*, 101, 110-123.
6. Neuzil, C.E., 2003, Hydromechanical coupling in geologic processes. *Hydrogeology Journa*l, 11, 41-83.
7. Rutqvist, J., Barr, D., Datta, R., Gens, A., millard, A., Olivella, S., Tsang, C.-F., Tsang, Y., 2005, Coupled thermal-hydrological-mechanical analysis of the Yucca Mountain Drift Scale Test-Comparision of field measurements to predictions of four different numerical models, *International Journal of Rock Mechanics & Mining Sciences*, 42, 680-697.
8. Rutqvist, J., Stephansson, O., 2003, The role of hydromechanical coupling in fractured rock engineering, *Hydrogeology Journal*, 11, 7-40.

9. Sato, T., Kikuchi, T., Sugihara, K., 2000, In-situ experiments on an excavation disturbed zone induced by mechanical excavation in neogene sedimentary rock at Tono mine, central Japan, *Engineering Geology*, 56, 97-108.
10. Sugihara, K., Matsu, H., Sato, T., 1999, In situ experiments on rock stress conditions and excavation disturbance in JNC's geoscientific research program in Japan, *Procedings of Internatonal Workshop Rock Mechanics of Nuclear Waste Repositories, 5-6 June, Veil, Colorado*, 159-183.
11. Tsang, C.-F., Bernier, F., Davies, C., 2005, Geohydromechanical processes in the excavation damaged zone in crystalline rock, rock salt, and indurated and plastic clays-in the context of radioactive waste disposal, *International Journal of Rcok Mechanics & Mining Sciences*, 42, 109-125.
12. Wang, J., Cook, P., Trautz, R., flexser, S., Hu, Q., Salve, R., Hudson, D., Conrad, M., Tsang, Y., Williams, K., Soll, W., Turin, J., 2001, *In-situ field testing of processes* ANL-NBS-HS-000005 REV01. Bechtel SAIC Co, Las Vegas, Navada.